Fatigue Properties of Copper Foil and the Evolution of Surface Roughness

Chung-Seog Oh[1,#], Jong-Sung Bae[1] and Hak-Joo Lee[2]

1 School of Mechanical Engineering, Kumoh National Institute of Technology, 1, Yangho-dong, Gumi-si, Gyeongbuk, South Korea, 730-701
2 Nano-Mechanical Research Division, Korea Institute of Machinery and Materials, 171, Jang-dong, Yuseong-gu, Daejeon, South Korea, 305-343
Corresponding Author / E-mail: ocs@kumoh.ac.kr, TEL: +82-54-478-7323, FAX: +82-54-478-7319

KEYWORDS: Copper foil, Fatigue, Closed-loop control, Mean stress, *S-N* curve, Surface roughness

The aim of this investigation was to extract the fatigue properties at the designated fatigue life of copper foil and observe the mean stress and stress amplitude effects on both the fatigue life and the corresponding surface morphology. Tensile tests were performed to determine the baseline monotonic material properties of the proportional limit and ultimate tensile strength. Constant amplitude fatigue tests were carried out using a feedback-controlled fatigue testing machine. The mean stress and the stress amplitude were changed to obtain the complete nominal stress-life curves. An atomic force microscope was utilized to observe the relationship between the fatigue damage and the corresponding changes in surface morphology. A Basquin's exponent of –0.071 was obtained through the fatigue tests. An endurance limit of 122 MPa was inferred from a Haigh diagram. The specimen surface became rougher as the number of fatigue cycles increased, and there was a close relationship between the fatigue damage and the surface roughness evolution.

Manuscript received: May 30, 2008 / Accepted: June 16, 2008

NOMENCLATURE

b = fatigue strength exponent or Basquin's exponent
C = fatigue strength coefficient
δ = grip-to-grip displacement
N = number of cycles to failure
P_a = load amplitude
P_m = mean load
R_a = average surface roughness
S = nominal stress
S_a = stress amplitude
S_e = fatigue limit under fully reversed loading
S_m = mean stress
S_{max} = peak/maximum stress
S_{PL} = proportional limit
S_t = ultimate tensile strength

1. Introduction

Copper (Cu) foil is widely used as an electrical conductor for flexible printed circuit boards (FPCBs) in mobile phones, laptop computers, etc., where they are exposed to fatigue loading due to repeated folding or sliding operations. The operations induce flexural as well as tensile stresses in the foil. The fatigue properties of the foil itself must be determined to guarantee product reliability during its design life.

Tension-tension, load-controlled fatigue results for aluminum[1] and electron beam evaporated copper[2] films were reported a decade ago. However, there has been a great deal of recent progress in fatigue test procedures as well improvements in the testing machines. Bagdahn and Sharpe[3] and Kim et al.[4] performed tension-tension fatigue tests for polycrystalline silicon. Most fatigue tests for thin films or foils are conducted under a predefined stress ratio and the data are arranged in terms of the peak/maximum stress in lieu of the stress amplitude and mean stress.

Han et al.[5] performed fatigue tests for two types of Cu foil made using rolling and electrodeposition processes, and showed that electrodeposited Cu had better fatigue resistance than rolled Cu. Park et al.[6] reported the results of tensile and high-cycle fatigue tests for copper film 15 μm thick and recommended the modified Goodman method when evaluating the fatigue life of thin films with mean stresses. Zhang et al.[7] showed that the fatigue damage behavior in Cu films 100 nm thick with nanometer-sized grains was different from that in micrometer-thick Cu films with large grains.

Casado et al.[8] performed quantitative analysis of the surface damage generated by fatigue of polyamide 6.6 reinforced with short fiber glass. They showed that the roughness became increasingly more marked as the number of cycles applied to the material increased. Yue[9] evaluated the surface roughness evolution under constant amplitude fatigue loading using crystal plasticity and reported that the roughness increased linearly with the number of fatigue cycles.

In this study, tension-tension fatigue tests and tensile tests were performed for electrodeposited Cu foil to extract the fatigue properties of the stress-life (*S-N*) curves, Basquin's exponent, and fatigue limit, and to observe any mean stress-dependent changes in the fatigue life. The fatigue properties from the tension-tension tests were used to develop a fatigue life estimation procedure for a

predefined mean stress and fatigue life. The surface roughness evolution was evaluated to determine the relationship between the roughness and the fatigue damage.

2. Research Procedure

The overall research processes are shown schematically in Fig. 1 to illustrate the contents of this paper.

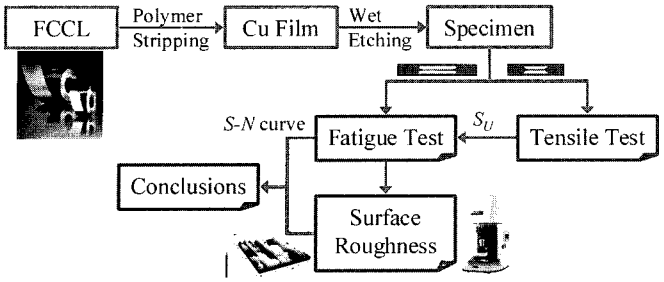

Fig. 1 Schematic diagram of the research procedure

3. Experimental Procedures

3.1 Specimens

A commercial single-sided flexible copper clad laminate (FCCL) was employed. The FCCL was composed of a polyimide (PI) layer 20 μm thick and an electrodeposited Cu layer 13 μm thick, as shown in Fig. 2.

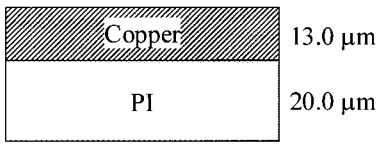

Fig. 2 Schematic structure of a single-sided FCCL

The foil specimens were designed by referencing the IEC[10] and ASTM[11] standards because there is no exact standard specimen at this scale. In particular, the curved portion between the gripped ends and the parallel section must have a sufficiently large radius of curvature not to fracture at the curved portion due to the stress concentration.[10] The specimens were formed by a wet etching process for the electrodeposited Cu foil. The PI layer was removed to leave just the copper film. The fabricated tensile and fatigue specimens were 600 μm in width, 13 μm in thickness, and 6.5 and 13 mm in length at the gage section, as shown in Fig. 3. The two side-supporting straps were cut just before testing.

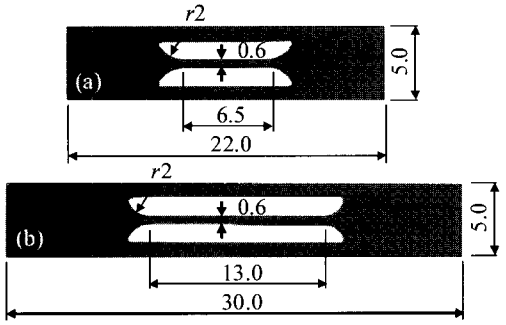

Fig. 3 (a) Tensile and (b) fatigue specimens [units: mm]

The surface of each specimen was ion-milled and observed with a focused ion beam (FIB, Nova 200 NanoLab; FEI Company). A typical texture is shown in Fig. 4 (a). The cross-sections were examined in a similar way; typical microstructures are shown in Fig. 4(b). The surface showed a few PI residues. The average grain sizes of the surface and cross-section, as determined following the test methods of ASTM E112,[12] were 1.44 ± 0.17 μm (mean ± standard deviation) and 1.43 ± 0.23 μm, respectively.

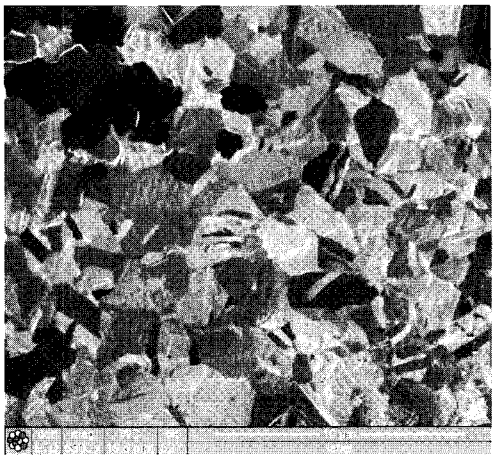

(a) Surface

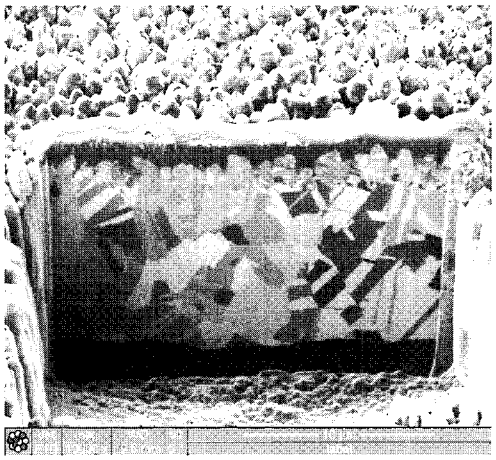

(b) Cross-section

Fig. 4 Microstructures of a Cu specimen

3.2 Test setup

A new closed-loop controlled tensile and fatigue testing machine (Nanodyn-DH; R&B) was used, as shown in Fig. 5. It was capable of load control as well as displacement control. The machine was composed of a linear motor, a 20 N load cell, translating stages, and a set of mechanical clamping grips. The part surrounding the specimen is enlarged and shown in the same figure to illustrate the grips in more detail. The grips had two fittings to make it easier to align the load train from the actuator to the load cell.

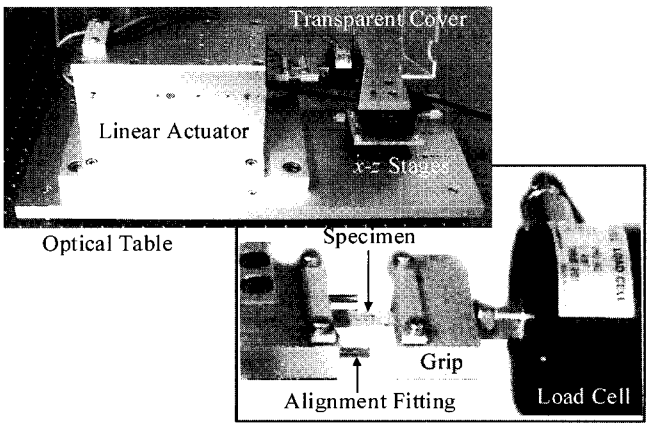

Fig. 5 Tensile and fatigue testing system

The control software (S/W) was programmed using Agilent VEE Pro (Version 7.5). The control S/W had almost the same features as a commercial large-scale testing system. The main functions of the S/W were actuator control, limit setting, cycle counting, data acquisition, and monitoring.

3.3 Test procedures

Tensile tests were performed to characterize the monotonic properties of the Cu foil. There was no need to measure the strain in the gage section because the proportional limit (*PL*, S_{PL}) and the ultimate tensile strength (*UTS*, S_U) were the only two mechanical properties of concern. The load and grip-to-grip displacement signals were recorded while the displacement was controlled. The loading speed was varied from 0.1 to 0.5 mm/min to determine the rate effect on the tensile properties. Three replicate tests were performed for each loading rate.

Constant amplitude fatigue tests were carried out at a frequency of 7 Hz in ambient air (25°C) while the load was controlled. The mean stress (S_m) and the stress amplitude (S_a) were varied to obtain the complete nominal stress-life (*S-N*) curves. The test conditions in terms of the mean load (P_m) and load amplitude (P_a) are listed in Table 1. The conversion factor from load [N] to stress [MPa] was 128.2. The numbers in the matrix represent the number of specimens tested. The fatigue life was defined as the life until complete rupture.

Table 1 Fatigue test matrix

P_a[N] \ P_m[N]	0.8	1.0	1.1	1.2
0.30				1
0.35				2
0.40		1	2	2
0.45		1^a	1	1
0.50	1^m	1^m	1^m	
0.55		1^a	2	
0.60	2	1^a		
0.65	1	1		
0.70	1			

Atomic force microscopy (AFM, XE-100; Park Systems) was used to measure the surface roughness of the specimens. The surface was scanned using the contact mode over a scan area of 45 × 45 μm^2. The average surface roughness (R_a)[13] was calculated over the entire scanned area. An as-received undamaged specimen was scanned 15 times to establish the baseline roughness. The regions near the fractured part were scanned to visualize the relationship between fatigue damage and surface roughness evolution. The superscripts "*a*" and "*m*" in Table 1 denote the specimens scanned to determine the effects of the stress amplitude and mean stress on the surface roughness, respectively.

4. Results and Discussion

4.1 Tensile test

Typical stress-displacement curves at each loading rate are shown in Fig. 6. Two types of displacement scale were used to observe the initial stress-displacement behavior in more detail. The start of the curve was nonlinear until the specimen was straightened. The two curves at loading rates of 0.1 and 0.3 mm/min showed almost identical behavior, but there was a slight deviation when the rate was 0.5 mm/min.

The ultimate tensile strength was determined by taking the maximum load measured in the test divided by the initial cross-sectional area (600 × 13 μm^2) of the specimen. The proportional limit was determined by superimposing a line with an identical slope as the linear portion of the stress-displacement relationship. The value of S_{PL} was taken as the last point before the constructed line and the stress-displacement relationship diverged. The measured monotonic properties are listed in Table 2.

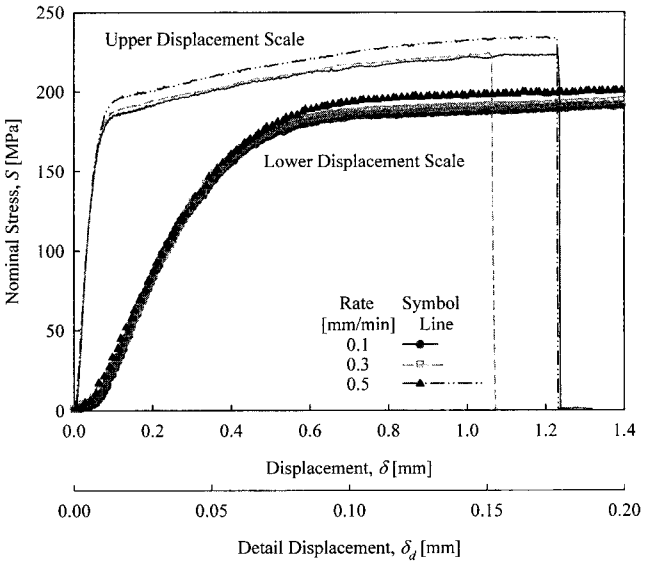

Fig. 6 Typical stress-displacement curves for each loading speed

Table 2 Tensile data: proportional limit and ultimate tensile strength

Properties [MPa] \ Loading Rate [mm/min]	0.1	0.3	0.5
S_{PL}	110	115	120
	120	117	120
	115	110	125
Mean ± 1σ	**114.5 ± 3.9**		121.7 ± 2.9
S_U	223.1	223.8	234.1
	226.8	224.4	226.9
	227.8	224.0	232.6
Mean ± 1σ	**225.0 ± 2.0**		231.2 ± 3.80

The tensile data at loading rates of 0.1 and 0.3 mm/min were almost the same; thus, statistical processing for both was performed together. This implies that the loading rate may be less than 0.3 mm/min when evaluating the tensile properties. From the table, the faster the loading rate, the higher the monotonic properties. In general, the yield strength and tensile strength will increase with increasing strain rate, although the effect on tensile strength is generally less pronounced.[14] This may be due to the mobility of dislocation. The dislocation movement will be more restricted at a higher loading rate, and thus the monotonic properties will be strengthened. The data obtained at a rate of 0.5 mm/min were excluded when calculating the monotonic properties. The value of S_{PL} was 114.5 MPa, while the value of S_U was 225 MPa. The *UTS* of 225 MPa is much lower than the value of 462 MPa reported in the literature[6] for a specimen of almost the same size and fabrication method (electrodeposition) measured following almost the same procedure. We assumed that the large discrepancy was due to the difference in current density in the electrodeposition process. Fritz *et al.*[15] reported that the mechanical strength and microstructure are strongly dependent on the mean current density used for electrodeposition. Usually, a high-strength film is obtained at a lower mean current density.

4.2 Fatigue test

The relationship between peak stress (S_{max}) and number of cycles to failure (*N*) is shown in Fig. 7 because fatigue test results were

arranged in terms of the maximum stress in many previous studies of thin films. There was no consistent relationship between the two parameters. The preferred use of S_{max} when arranging fatigue data is due to the lack of closed-loop fatigue testing machines capable of amplitude and mean load control for thin films or foils. It is worth noting that the peak stresses fell above the yield stress, even in the high-cycle regime of 10^5 cycles or more. Judelewicz et al.[16] studied the microstructural development during the fatigue of copper foils 10 to 100 μm thick, and showed that thinner specimens have higher cycle numbers at the same stress amplitude for samples with grain sizes comparable with the sample thickness.

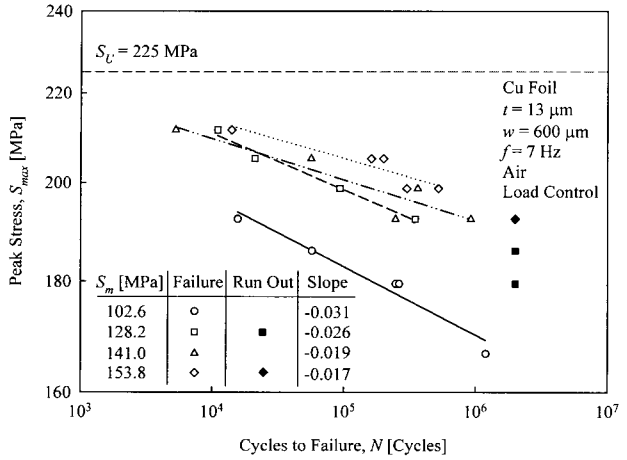

Fig. 7 Peak stress *vs.* cycles to failure

The *S-N* curves were rearranged in terms of the stress amplitude and mean stress instead of the maximum stress, as shown in Fig. 8. There was a clear linear relationship between log (S_a) and log (N) for each mean stress, leading to Basquin's equation,[11]

$$S_a = CN^b \tag{1}$$

where b is the fatigue strength exponent (Basquin's exponent) and C is fatigue strength coefficient. The fatigue strength exponent is the slope of the curves in Fig. 8, and is listed in the same figure. The mean slope of –0.071 appears reasonable as the exponent usually varies between –0.05 and –0.12 for most metals.[17] The exponent was almost the same as that of 33-μm-thick wrought Cu film[18] and bulk Cu,[19] but slightly lower than the value of –0.09 reported by Park et al.[6]

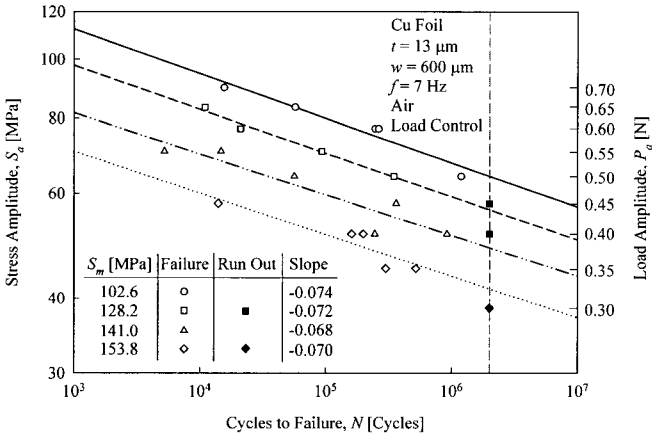

Fig. 8 Stress amplitude *vs.* cycles to failure for each mean stress

The alternating stresses corresponding to a life of 2×10^6 cycles were calculated by extrapolating the individual *S-N* curves and reading the intersection points between the curves and the life of the 2×10^6 line, represented by the red dashed line in Fig. 8. A Haigh diagram was constructed using the mean and alternating stresses as shown in Fig. 9. There are 5 data points in the figure. Linear curve fitting was performed and the curve was extrapolated to find the fatigue limit (S_e) under zero mean stress, which is the fully reversed loading condition. We inferred that the fatigue limit under fully reversed loading was about 122 MPa. This procedure was based on the following modified Goodman equation:

$$\frac{S_a}{S_e} + \frac{S_m}{S_u} = 1 \tag{2}$$

The fatigue strength exponent and the fatigue limit corresponding to a life of 2×10^6 cycles are important to produce a durable design for FPCBs. This study has established a methodology to obtain these fatigue properties for foils or films.

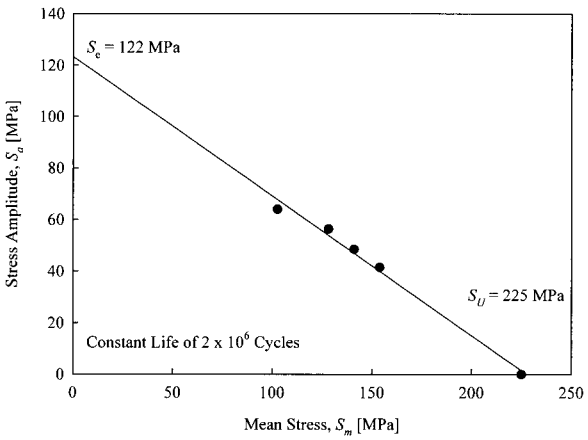

Fig. 9 Haigh diagram for Cu foil

4.3 Surface roughness evaluation

An as-received undamaged specimen was first scanned 15 times to establish the baseline roughness value. The mean and standard deviations of the average roughness were 156 and 13 nm, respectively. One of the 15 scanned images is shown in Fig. 10.

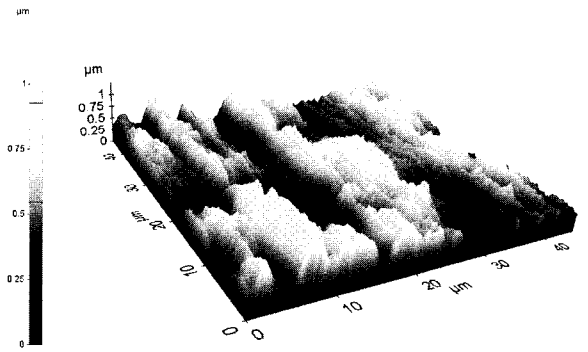

Fig. 10 AFM image of an undamaged specimen

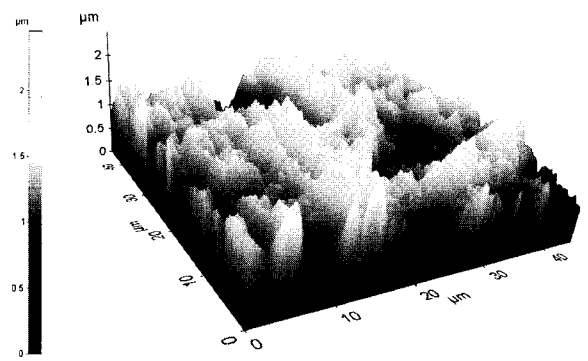

Fig. 11 AFM image of a damaged specimen under 1.2 ± 0.35 N

An AFM image of a failed specimen (N_f = 300,697 cycles) under a loading of 1.2 ± 0.35 N is shown in Fig. 11 to provide a clear comparison with Fig. 10. The scale factors for both images are equivalent. The damaged surface was rougher than the undamaged surface. We assumed that the fatigue loading introduced plastic deformation in the material, which accumulated as the loading was repeated.

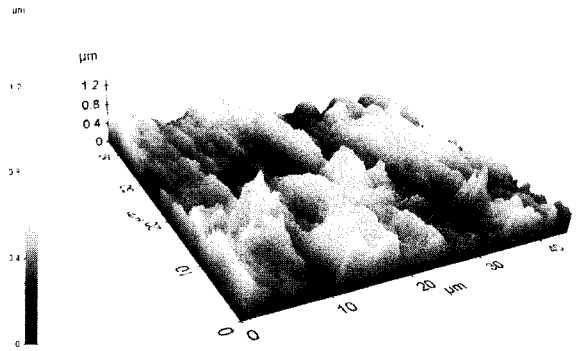

Fig. 12 AFM image of a run out specimen under 1 ± 0.45 N

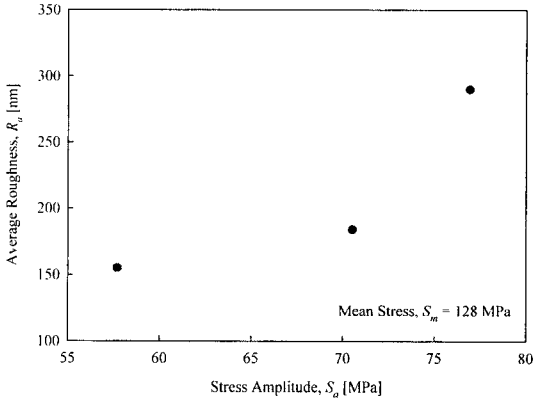

Fig. 13 Average roughness *vs.* stress amplitude

The R_a value of a specimen that did not fail before 2×10^6 cycles under a loading of 1 ± 0.45 N was almost the same as that of an undamaged specimen. This observation indicated that there was little damage at lower stress levels. An AFM image of this run-out specimen is shown in Fig. 12. The images in Figs. 10 and 12 are similar.

The R_a of a specimen after a fatigue test was evaluated to determine the effects of the mean stress and stress amplitude on the surface morphology. The R_a values for mean loads of 0.8, 1.0, and 1.1 N under a constant load amplitude of 0.5 N were 158, 189, and 180 nm, respectively. Thus, a higher mean stress made the surface rougher. The R_a values for load amplitudes of 0.45, 0.55, and 0.6 N at a mean load of 1 N were 155, 184, and 290 nm, respectively. The average roughness as a function of the stress amplitude is shown in Fig. 13. Greater alternating stress induced a greater surface roughness.

It is worth noting that the surface roughness can be a footprint for damage to a material. The stress level suffered by a film during its service may be inferred from surface roughness measurements of a fractured specimen. However, the surface of the as-received specimens in this study was too rough to evaluate the amount of damage quantitatively. More extensive tests with very smooth specimens are required to draw more reliable and valuable conclusions. In addition, a fatigue test for the FCCL itself is required to correlate the Cu foil material properties with those of FCCL.

5. Conclusions

Tensile and fatigue tests were conducted to extract the mechanical properties of Cu foil. Special emphasis was placed on the effects of the mean stress and stress amplitude on the fatigue life and the corresponding surface morphology changes. AFM was used to determine the relationship between fatigue damage and surface roughness. The preliminary findings can be summarized as follows.

(1) The loading speed must be less than 0.3 mm/min when measuring the tensile properties of Cu foils 13 μm thick.
(2) The proportional limit was 114.5 MPa and the tensile strength was 225 MPa.
(3) The *S-N* curve of Cu foil was obtained using a closed-loop load control. A fatigue strength exponent of –0.071 was obtained.
(4) The fatigue limit corresponding to a life of 2×10^6 cycles under fully reversed loading of 122 MPa was inferred from a Haigh diagram based on the modified Goodman equation.
(5) There was a close relationship between the fatigue damage and the surface morphology. The surface morphology was greatly influenced by the stress amplitude but only slightly influenced by the mean stress.

ACKNOWLEDGMENT

This research was supported by research fund of the Kumoh National Institute of Technology. We thank Dr. S.-W. Han of KIMM for supplying the specimens.

REFERENCES

1. Read, D. T. and Dally, J. W., "Fatigue of Microlithographically-Patterned Free-Standing Aluminum Thin Film under Axial Stresses," J. Electronic Packaging, Vol. 117, No. 1, pp. 1-5, 1995.
2. Read, D. T., "Tension-tension Fatigue of Copper Thin Films," Int. J. Fatigue, Vol. 20, No. 3, pp. 203-209, 1998.
3. Bagdahn, J. and Sharpe, W. N., "Fatigue of Polycrystalline Silicon under Long-term Cyclic Loading," Sens. Actuators, Vol. A103, No. 1/2, pp. 9-15, 2003.
4. Kim, S.-W., Oh, C.-S. and Lee, H.-J., "Specimen Aligning Techniques in Tensile and Fatigue Tests for Thin Films," Fatigue Fract. Engng Mater. Struct., Vol. 30, No. 1, pp. 64-71, 2007.
5. Han, S.-W., Seo, K.-J., Kim, W.-D., Lee, H.-J., Lee, H.-W., Shin, J.-H. and Lee., J.-J., "Fatigue Behavior of Thin Cu Foils for Flexible Printed Circuit Board," Solid State Phenomena, Vol. 124-126, pp. 1369-1372, 2007.
6. Park, J.-H., An, J.-H., Kim, Y.-J., Huh, Y.-H. and Lee, H.-J., "Tensile and High Cycle Fatigue Test of Copper Thin Film," Mat.-wiss. u. Werkstofftech., Vol. 39, No. 2, pp. 187-192, 2008.
7. Zhang, G. P., Sun, K. H., Zhang, B., Gong, J., Sun, C. and Wang, Z. G., "Tensile and Fatigue Strength of Ultrathin Copper Films," Mat. Sci. & Engng., Vol. A483-484, pp. 387-390, 2008.
8. Casado, J. A., Gutierrez-Solana, F., Polanco, J. A. and Carrascal, I., "The Assessment of Fatigue Damage on Short-Fiber-Glass Reinforced Polyamides (PA) through the Surface Roughness Evolution," Polym. Compos., Vol. 27, No. 4, pp. 349-359, 2006.
9. Yue, Z. F., "Surface Roughness Evolution under Constant Amplitude Fatigue Loading using Crystal Plasticity," Engng Fract. Mech., Vol. 72, No. 5, pp. 749-757, 2005.
10. "Semiconductor Devices – Micro-electromechanical Devices – Part 3: Thin Film Standard Test Piece for Tensile Testing," IEC 62047-3 Ed. 1.0, 2006.

11. "Standard Test Methods of Tension Testing of Metallic Foil," ASTM Standards, Vol. 03.01, E345-93, ASTM, pp. 2, 2002.

12. "Standard Test Methods for Determining Average Grain Size," ASTM, Vol. 03.01, E112-96, pp. 4-14, 2002.

13. Sharma, V. S, Dhiman, S., Sehgal, R. and Sharma, K., "Assessment and Optimization of Cutting Parameters while Turning AISI 52100 Steel," Int. J. Precision Engineering and Manufacturing, Vol. 9, No. 2, pp. 54-62, 2008.

14. "Standard Test Methods for Tension Testing of Metallic Materials," ASTM, Vol. 03.01, E8M-00, pp. 19, 2002.

15. Fritz, T., Cho, H. S., Hemker, K. J., Mokwa, W. and Schnakenberg, U., "Characterization of Electroplated Nickel," Microsystem technologies: sensors, actuators, systems integration, Vol. 9, No. 1/2, pp. 87-91, 2002.

16. Judelewicz, M., Kunzi, H.-U., Merk, N. and Ilschner, B., "Microstructural Development during Fatigue of Copper Foils 20-100 μm thick," Mater. Sci. Eng. A, Vol. 186, No. 1/2, pp. 135-142, 1994.

17. Bannantine, J. A., Corner, J. J. and Handrock, J. L., "Fundamentals of Metal Fatigue Analysis," Prentice Hall, pp. 1-10 & 59-66, 1990.

18. Hong, S. and Weil, R., "Low Cycle Fatigue of Thin Copper Foils," Thin Solid Films, Vol. 283, No. 1/2, pp. 175-181, 1996.

19. Lukas, P. and Klesnil, M., "Cyclic Stress-Strain Response and Fatigue Life of Metals in Low Amplitude Region," Mat. Sci. Eng., Vol. 11, No. 6, pp. 345-356, 1973.